

Revealing the Pseudocapacitance Charge Storage Mechanism of Sulfur-Doped Carbon Supercapacitors in Non-Aqueous Electrolyte through *in situ* EPR

Tobias Neff^{1,2#}, Friedrich Stemmler^{3#}, Leonhard Kolb², Joris van Slageren³, Anke Krueger^{1*}

¹Institute of Organic Chemistry, University of Stuttgart, Pfaffenwaldring 55, 70569 Stuttgart, Germany, ²Institute for Organic Chemistry, Julius-Maximilian University Würzburg, Am Hubland, 97074 Würzburg, Germany,

³Institute of Physical Chemistry, Pfaffenwaldring 55, 70569 Stuttgart, Germany

#equal contribution, *anke.krueger@oc.uni-stuttgart.de

Supporting Information

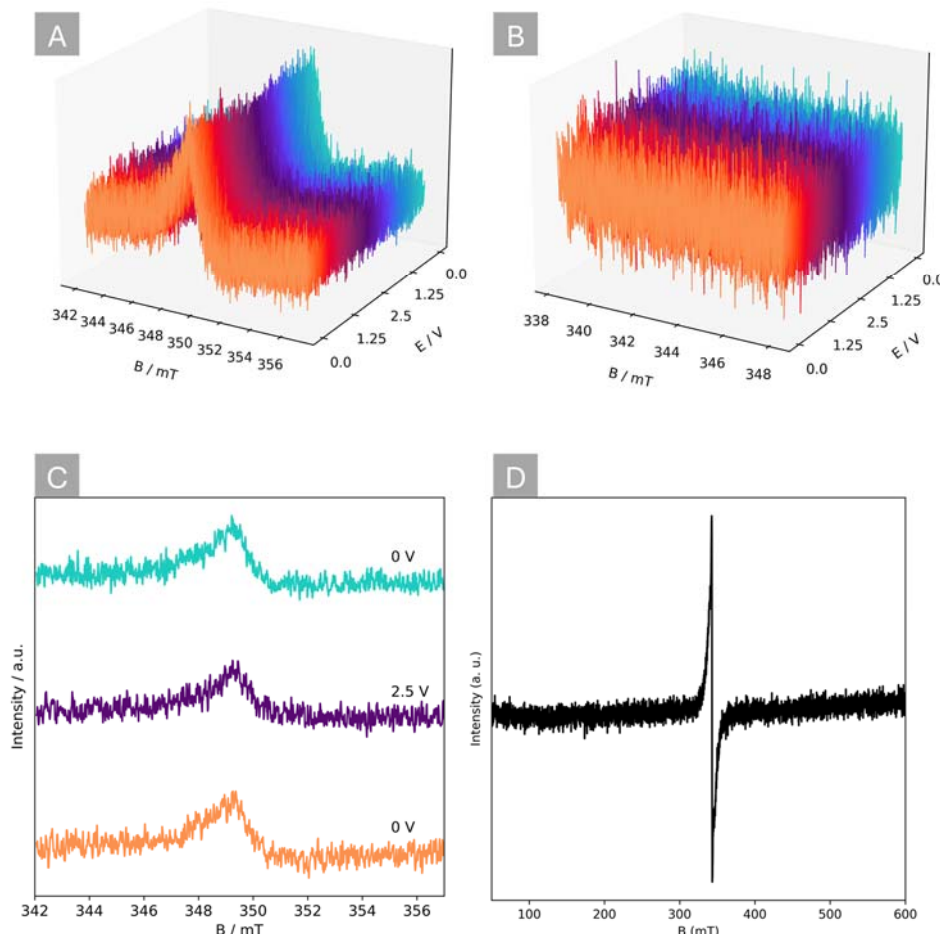


Fig. S1: *In situ* EPR measurements at 1 mW and 3 G for (A) pure OLC and (B) CMC binder. OLC exhibits a weak paramagnetic signal with a high signal-to-noise ratio and minimal changes during the measurement. In contrast, CMC binder shows no detectable paramagnetic signal, which proves its non-paramagnetic nature and therefore excludes an influence on the measurement. (C) Individual ESR spectra of OLC recorded at selected voltages, showing no significant differences during the charging process. (D) EPR spectrum of dry OLC powder displays a single signal likely associated with highly localized defects, like those observed in graphene.[S1]

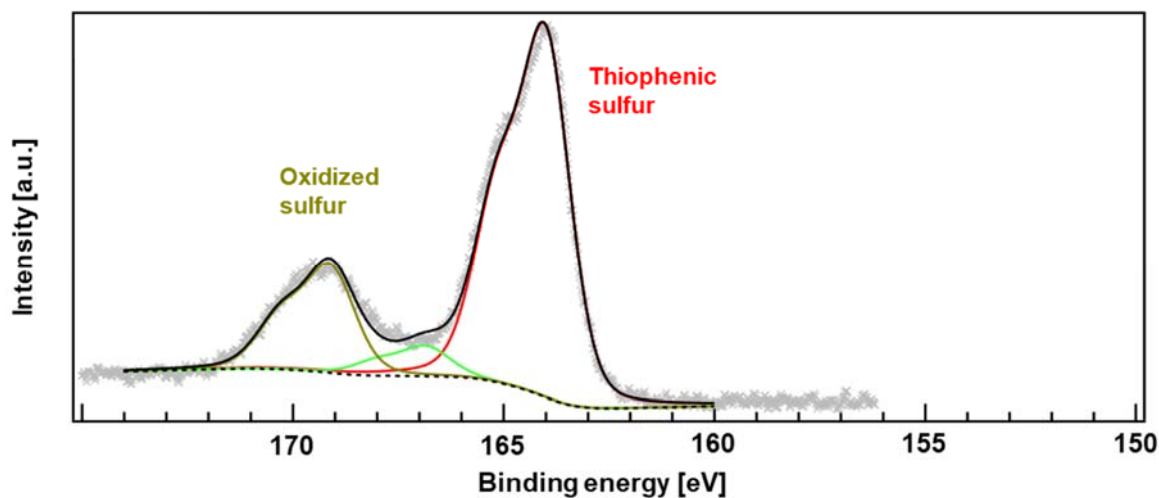


Fig. S2: XPS spectrum of the $S2p$ orbital, revealing thiophenic and oxidized sulfur. The same batch of material was used in a previous work, in which a detailed XPS analysis was conducted. The figure was reused under licence *CC BY 4.0* from *ref.[S2]*

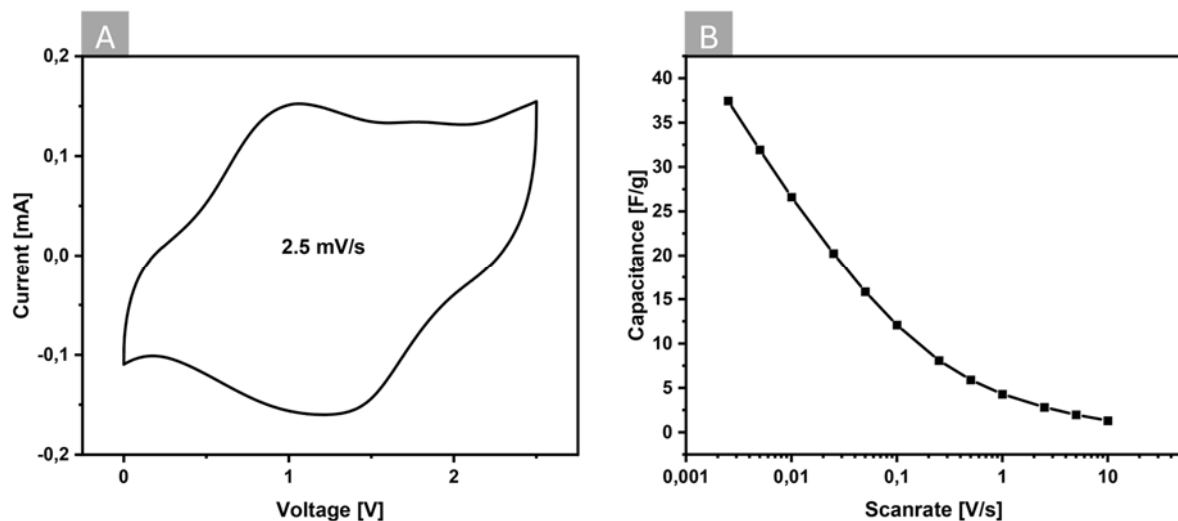


Fig. S3: Electrochemical performance of pure sulfur doped carbon: **(A)** Cyclic voltammogram at 2.5 mV/s, displaying broad redox peaks and no rectangular shape. This is indicative of a high amount of pseudocapacitance. **(B)** Capacitance as a function of scan rate, showing a drastic decay: only ~10% of the initial value remains at 5 V/s.

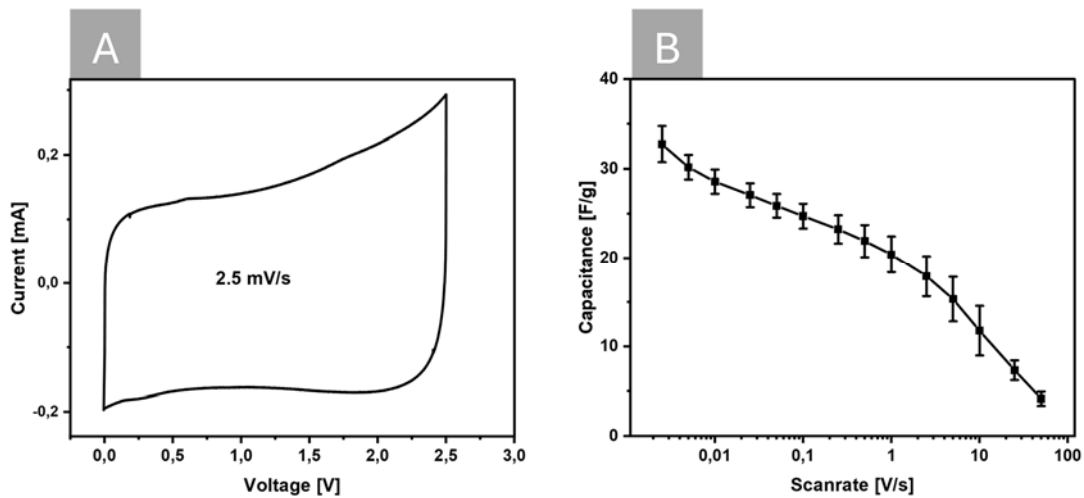


Fig. S4: Electrochemical performance of OLC: **(A)** Cyclic voltammogram at 2.5 mV/s, displaying a nearly rectangular shape without redox peaks indicative of pure supercapacitive behaviour. **(B)** Capacitance as a function of scan rate, showing high capacitance values maintained at scan rates up to 5 V/s.

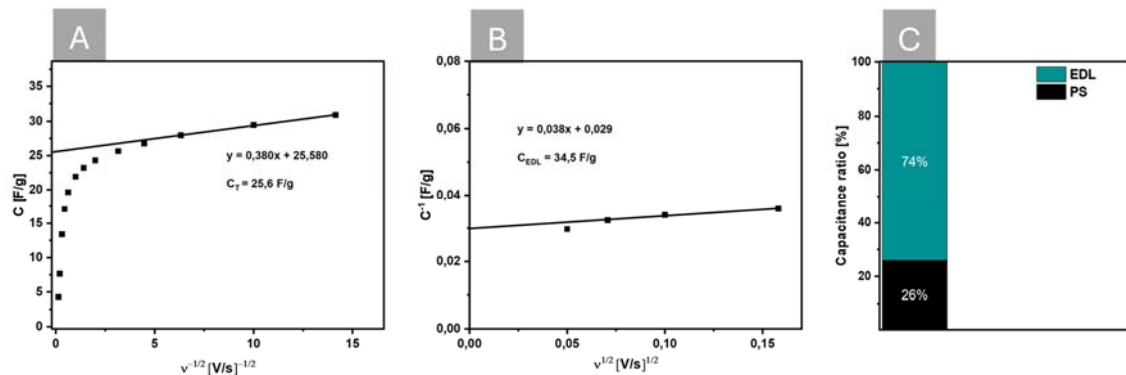


Fig. S5: Electrochemical analysis of OLC using the Trasatti method. **(A)** Trasatti plot illustrating the extrapolated total capacitance and **(B)** showing the proportion of EDL capacitance. **(C)** Ratio of pseudocapacitive to EDL charge contributions, confirming that OLC exhibits predominantly EDL behaviour with minimal pseudocapacitive contribution.

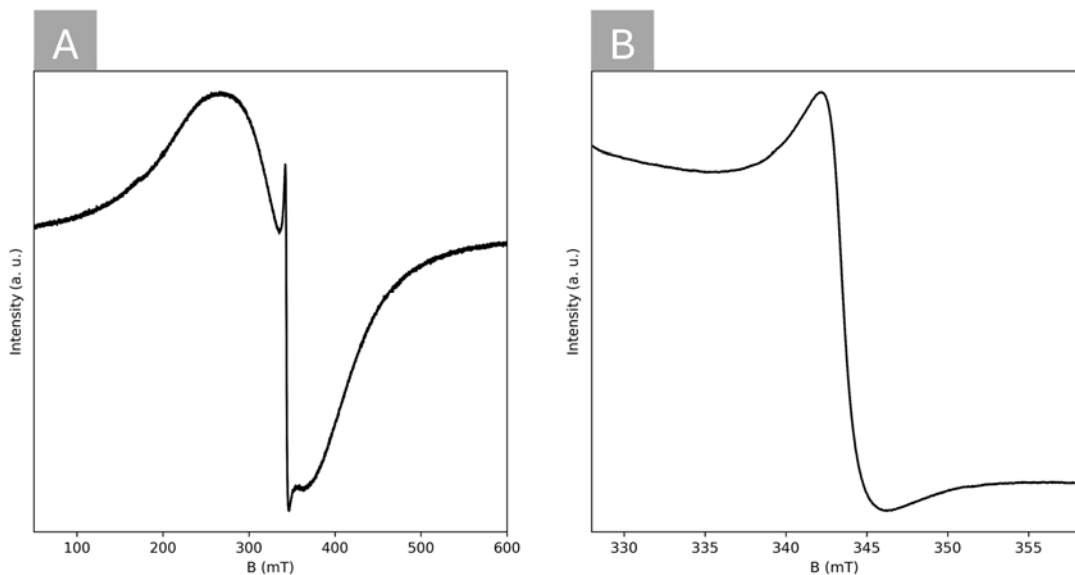


Fig. S6: Electron spin resonance analysis of sulfur-doped carbon powder after synthesis, measured at 1 mW with no voltage applied: **(A)** 3 G EPR spectrum showing high asymmetry. **(B)** Detailed scan of the $g = 2$ region, highlighting the spectral features of the material.

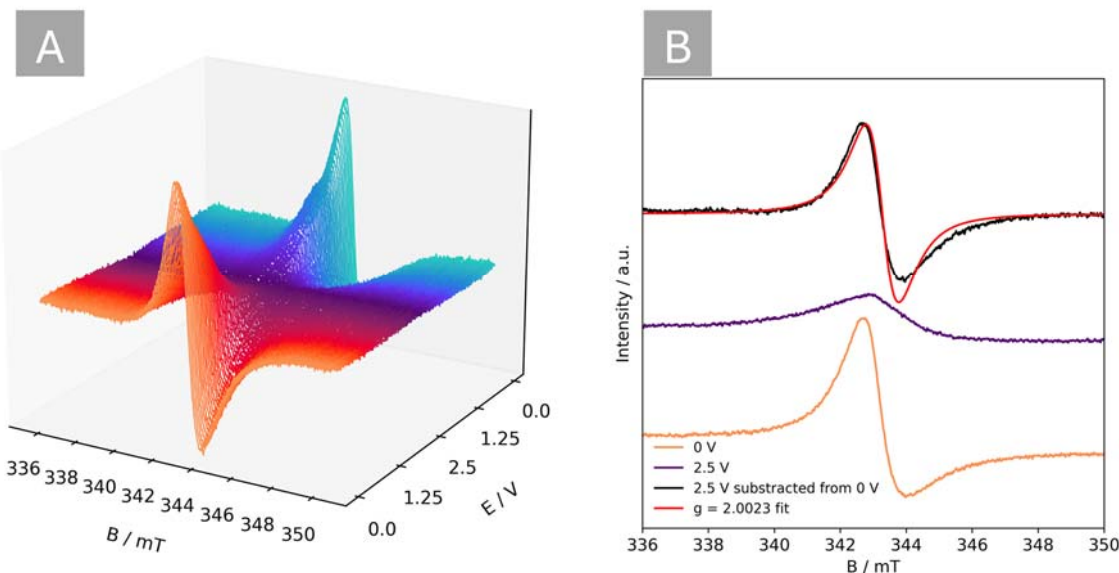


Fig. S7: **(A)** Subtraction of the purely Dysonian EPR spectrum measured at 2.5 V from all other recorded spectra displays the evolution of the voltage dependent Lorentzian signal. **(B)** Fit of the residual signal gives a g value of $g = 2.0023$.

References

[1] O.V. Yazyev, M.I. Katsnelson, Magnetic Correlations at Graphene Edges: Basis for Novel Spintronics Devices, *Physical Review Letters* 100(4) (2008) 047209. <https://doi.org/10.1103/PhysRevLett.100.047209>

[2] T. Neff, J. Heßdörfer, A. Bilican, L. Kolb, F. Reinert, A. Krueger, Superior Sulfur-Doped Carbon Anodes for Sodium-Ion Batteries through Incorporation of Onion-Like Carbon, *Electrochimica Acta* (2025) 146912. <https://doi.org/10.1016/j.electacta.2025.146912>